International Immunology, Vol. 17, No. 5, pp. 569–579
doi:10.1093/intimm/dxh236

Neutralization of chemokines RANTES and MIG increases virus antigen expression and spinal cord pathology during Theiler's virus infection

Daren R. Ure[1,4], Thomas E. Lane[2], Michael T. Liu[2] and **Moses Rodriguez[1,3]**

[1]Department of Immunology and [3]Department of Neurology, Mayo Foundation and Graduate School, 428 Guggenheim Building, 201 1st Street SW, Rochester, MN 55905 USA
[2]Center for Immunology and Department of Molecular Biology and Biochemistry, University of California, Irvine, CA 92612-3900, USA

[4]Present address: Isotechnika, Inc., 5120, 75th Street, Edmonton, Alberta T6E 6W2 Canada

Keywords: chemokines, demyelination, interleukins, virus persistence

Abstract

The role of chemokines during some viral infections is unpredictable because the inflammatory response regulated by these molecules can have two, contrasting effects—viral immunity and immunopathologic injury to host tissues. Using Theiler's virus infection of SJL mice as a model of this type of disease, we have investigated the roles of two chemokines—regulated on activation, normal T cell-expressed and secreted (RANTES) chemokine and monokine induced by IFN-γ (MIG)—by treating mice with antisera that block lymphocyte migration. Control, infected mice showed virus persistence, mild inflammation and a small degree of demyelination in the white matter of the spinal cord at 6 weeks post-infection. Treatment of mice with RANTES antiserum starting at 2 weeks post-infection increased both viral antigen expression and the severity of inflammatory demyelination at 6 weeks post-infection. MIG antiserum increased the spread of virus and the proportion of spinal cord white matter with demyelination. Overall, viral antigen levels correlated strongly with the extent of pathology. At the RNA level, high virus expression was associated with low IL-2 and high IL-10 levels, and RANTES antiserum decreased the IL-2/IL-10 ratio. Our results suggest that RANTES and MIG participate in an immune response that attempts to restrict viral expression while limiting immunopathology and that anti-chemokine treatment poses the risk of exacerbating both conditions in the long term.

Introduction

Infection of susceptible SJL mice intracranially with Theiler's murine encephalomyelitis virus (TMEV) virus induces a biphasic disease. The first phase is characterized by transient encephalitis within the first 2 weeks of infection due to rapid viral replication in the brain. In the second phase the virus moves to the spinal cord at 7–14 days post-infection (d.p.i.) and establishes lifelong infection in the white matter of the cord. The Daniel's strain (DA) of TMEV persists within oligodendrocytes, astrocytes and macrophages/microglia. Viral persistence results in chronic inflammation by lymphocytes and macrophages, as well as activation of central nervous system (CNS) glia, which leads to extensive demyelination, axonal degeneration and progressive neurological deficits starting at 2–3 months post-infection.

Theiler's virus induces the production of a variety of chemokines in the CNS—molecules that regulate migration and function of inflammatory cells. Similar patterns of chemokine expression develop in the CNS after infections with different strains of TMEV and with other viruses (1–11). Some of the major chemokines are regulated on activation, normal T cell-expressed and secreted chemokine (RANTES; CCL5), monokine induced by IFN-γ (MIG; CXCL9), interferon-γ inducible protein-10 (IP-10; CXCL10), monocyte chemotactic protein-1 (MCP-1; CCL2), macrophage inflammatory protein-1α (MIP-1α; CCL3) and MIP-1β (CCL4). Most are up-regulated within several days of infection and remain elevated as long as viral infection and/or tissue injury persists. A primary role for these chemokines is to facilitate infiltration of virus-reactive

Correspondence to: M. Rodriguez; E-mail: rodriguez.moses@mayo.edu

Received 24 February 2004, *accepted* 7 February 2005

Transmitting editor: M. Miyasaka

Advance Access publication 11 April 2005

lymphocytes. For example, lymphocyte infiltration promoted by MIG and IP-10 during mouse hepatitis virus (MHV) infection serves to limit viral replication and reduce mortality (12–14). In contrast, inflammatory responses also potentially are injurious to normal tissues, and therefore under some conditions chemokine production could be harmful. Theiler's virus infection of SJL mice is one such example where the role of chemokines cannot be easily predicted because the inflammatory response has two prominent and contrasting effects. CD4 and CD8 lymphocytes are necessary for preventing mortality throughout infection, but their infiltration into the CNS over the long term also leads significantly to myelin and axonal destruction. Antiviral responses in SJL mice are insufficient to clear virus, at least in part due to a lack of virus reactivity of most infiltrating lymphocytes (15). Therefore, virus and the resulting inflammatory response persist lifelong in the spinal cord. The secondary development of autoreactivity might also play a role in chronic disease (16). Thus, chemokines probably exert both positive and negative effects concurrently in this model.

The two chemokines that we investigated in the present study were RANTES and MIG. Our protocol was to treat mice with one or two doses of neutralizing antiserum to either of these chemokines and examine the effects on viral load, cytokine mRNAs and spinal cord pathology 1 month later. In designing this protocol, our primary focus was spinal cord pathology because the degree of motor dysfunction correlates strongly with the extent of spinal cord injury (17, 18). Since CNS injury is a long-term manifestation of infection, a sufficiently long treatment period was required to detect changes in pathology if they developed. Moreover, by limiting the number of antiserum treatments we attempted to reduce immunopathology without significantly affecting virus load. Indeed, we found that virus expression increased only slightly, but counter to our hypothesis, spinal cord pathology also increased rather than decreased by 1-month post-treatment.

Methods

Mice and experimental design

Six- to eight-week old SJL/J mice (Jackson Laboratories, Bar Harbor, ME, USA) were intra-cerebrally injected with 2.0×10^6 plaque-forming unit (p.f.u.) of Daniel's strain of TMEV. At the described times mice were injected intra-peritoneally with 0.5 ml chemokine antiserum (provided by Tom Lane) or normal goat serum (Sigma, St Louis, MO, USA). Chemokine antisera were made by injection of rabbits (for MIG antiserum) or goats (for RANTES antiserum) with peptide–keyhole limpet hemocyanin conjugates corresponding to the specific chemokines. The antisera reacted specifically with the cognate chemokines and blocked CD4 and CD8 lymphocyte migration *in vivo* in previous studies (7, 14, 19, 20). The antibodies also were expected to be efficacious during Theiler's virus infection because Ig delivered systemically are detectable in the CNS (21, 22). We estimate that a single injection resulted in a neutralizing antibody concentration of 0.25 mg ml^{-1}, based on an approximate blood volume of 2 ml per mouse. All animal protocols were approved by the Mayo Institutional Animal Care and Use Committee.

Three separate experiments were conducted. In each experiment mice were treated with chemokine antiserum (anti-RANTES or anti-MIG) or normal goat serum once or twice (separated by 7 days) starting at 10 d.p.i. Analyses of RNA levels, virus expression and pathology were conducted 1 month following the last antiserum treatment. Data from multiple experiments were combined because single and double antiserum administrations were considered to have similar effects. Single antibody injections are sufficient to neutralize target antigens *in vivo* (23), and the effective antibody concentration in the serum was unlikely to be significantly prolonged by a second injection (1–3 week Ig half-life), compared with the 4-week span of each experiment. The relatively late analysis was chosen to be able to detect possible changes in spinal cord pathology, which typically manifest many days or weeks following immunomodulatory treatments. In the Theiler's virus model we typically observe no mortality beyond 10 d.p.i., and functional deficits do not become obvious until ~3 months post-infection. Treatment with either chemokine antiserum neither increased mortality nor induced functional deficits.

Antiserum-neutralizing activity

In vitro chemotaxis assays were used to demonstrate chemokine-neutralizing activity of anti-MIG and anti-RANTES antiserum. For anti-MIG, 5×10^5 $CXCR3^+$ 300-19 lymphocytic cells (generously provided by B. Moser) were re-suspended in RPMI + 1% FBS and placed in the top chamber of a Multiscreen-MIC S510 transwell plate (96-well, 5μM pore size; Millipore, Billerica, MA, USA). The bottom well contained either recombinant mouse MIG (Biosource, Camarillo, CA, USA) 200 ng ml^{-1} alone or recombinant mouse MIG (200 ng ml^{-1}) pre-incubated with anti-MIG antisera at varying concentrations (200, 100, 50 ug ml^{-1}). All samples were performed in duplicate. For anti-RANTES determination, splenocytes were isolated from mice that had been immunized with MHV (2×10^5 p.f.u.) 7 days prior and expressed CCR5, a RANTES receptor (24, 25). A total of 5×10^5 splenocytes were re-suspended in RPMI + 1% FBS and chemotaxis was determined as above using recombinant mouse RANTES (Biosource) and anti-RANTES antisera in place of MIG and anti-MIG antisera. Assay plates were incubated at 37°C for 2 h and migration was determined by counting the number of cells in the bottom well in five random high power fields (×200) for each sample. Migration is presented as a chemotactic index that is calculated by dividing the number of cells that migrated in response to signal by the number of cells responding to medium alone (26).

Pathologic analysis

Mice were over-dosed with sodium pentobarbital and perfused by intra-cardiac puncture with Trump's fixative. Spinal cords were removed and analyzed on coded sections as follows:

(i) Spinal cord lesion frequency: Dissected spinal cords were cut into 1-mm blocks, and every third block was embedded in glycol methacrylate. Coronal, cross-sections were stained with a modified erichrome stain with a cresyl violet counterstain to demonstrate demyelination and

inflammation, as previously described (27). Lesions were quantified by determining the percentage of spinal cord quadrants (four possible quadrants per section) showing any sign of pathology from an average of 10 sections per spinal cord.

(ii) Spinal cord lesion severity: Lesion severity was assessed from coded, spinal cord sections (prepared above) without knowledge of experimental group. Each spinal cord quadrant showing pathology was scored according to the following 4-point scale: Grade 1 = mild lymphocyte infiltration; Grade 2 = mild lymphocyte and macrophage infiltration and minimal demyelination; Grade 3 = moderate inflammation and demyelination; Grade 4 = extensive inflammation, demyelination and severe tissue damage.

All analyses were done without knowledge of the treatment groups.

Immunostaining and virus antigen quantitation

Alternate blocks from the same, Trump's-fixed spinal cords as for pathologic analyses, were embedded in paraffin. Cross-sections were collected for immunostaining virus antigen with polyclonal, rabbit antiserum to purified DA virus (28) followed by biotinylated, secondary antibodies and ABC reagent (Vector Laboratories, Burlingame, CA, USA). Viral antigen expression was measured as the percentage of spinal cord quadrants with infected cells and by the total number of infected cells relative to the total cross-sectional area examined. Cross-sectional areas were measured using a ZIDAS interactive camera lucida system attached to a Zeiss photomicroscope. Ten sections from each spinal cord were analyzed for virus expression, and sections were analyzed without knowledge of experimental group.

Immunostaining for CD4 and CD8 T cells was performed on cryosections from freshly frozen spinal cords from additional mice. Cells were detected using CD4 and CD8 mAbs (BD-Pharmingen, San Diego, CA, USA), followed by biotinylated, secondary antibodies and ABC reagent (Vector Laboratories).

Real-time reverse transcriptase–PCR

Spinal cords and brain stems were collected immediately after over-dosing mice with sodium pentobarbital. Total RNA was isolated using RNA STAT-60 (Tel-Test Inc., Friendswood, TX, USA) and stored at −80°C. RNA levels were determined by real-time reverse transcriptase (RT)–PCR using a LightCycler instrument (Roche Diagnostics, Mannheim, Germany) and Qiagen QuantiTect RT–PCR (SYBR Green) kits (Valencia, CA, USA). Primer sequences are shown in Table 1. Standard curves for quantifying sample RNA were generated from plasmids containing the complete cDNA sequences for the specific genes. Cloning of PCR-amplified cDNAs was performed with Promega pGEM-T Easy kits and DH5α (Library grade) *Escherichia coli*. Plasmids from positive transformants were isolated with Qiagen Miniprep spin columns. Standards were amplified with the same reaction mixtures and conditions as the experimental samples and had single melting peaks and linear product-cycle regressions over a 5-log range of input plasmid. Twenty nanograms of total sample RNA was used in each reaction, an amount found in titration experiments to be optimal for detecting differences in RNA levels. Reaction conditions were as follows:reverse transcription 50°C for 20 min, denaturation 95°C for 15 min, amplification (35 cycles) 95°C for 10 s + 57°C for 10 s + 72°C for 15 s and melt 0.1°C s^{-1}. Reaction controls included water alone or experimental samples made through mock RNA isolation (tissue excluded). No specific reaction product was amplified in control reactions, as indicated by melting curves and electrophoresis. Experimental samples that gave reaction products with melting peaks lower than those expected (e.g. water reaction) were considered below the limit of detection.

Statistics

Each experimental group was compared individually with the appropriate control group and statistically significant differences were determined by non-parametric Student's *t* test (Mann–Whitney) with significance set at $P \leqslant 0.05$. Correlations were determined using the Spearman non-parametric coefficient.

Results

Neutralizing activity of chemokine antiserum

The roles of RANTES and MIG during early stages of Theiler's virus infection were investigated using neutralizing, rabbit or goat antisera. These antisera were shown previously to reduce lymphocyte infiltration and disease course in a tumor model and during MHV infection (7, 19, 20). The neutralizing activities were confirmed using *in vitro* chemotaxis assays. Cells responsive to RANTES (splenocytes from MHV-infected mice) or MIG (300-19 cell line) were seeded into the upper chamber of transwell plates, and recombinant chemokines and antisera were placed in the bottom chamber. Cell migration into the bottom chamber was induced by the presence of the chemokines. Anti-MIG antiserum reduced cell migration by a maximum of 75%, whereas anti-RANTES blocked migration completely (Fig. 1). Thus, these antisera neutralized most or all chemokine-specific activity.

Table 1. RT–PCR primer sequences

Gene	Forward primer	Reverse primer
VP2	5′-TGGTCGACTCTGTGGTTACG-3′	5′-GCCGGTCTTGCAAAGATAGT-3′
GAPDH	5′-CCATGTTTGTGATGGGTGTG-3′	5′-GATGCAGGGATGATGTTCTG-3′
CXCR3	5′-AACTCTTCCATTGTGGGCAG-3′	5′-AAGGCCCCTGCATAGAAGTT-3′
IL-2	5′-GCAGGCCACAGAATTGAAAG-3′	5′-TCCACCACAGTTGCTGACTC-3′
IL-10	5′-GCCTTGGGAAGCAATTGAAG-3′	5′-AACTGGCCACAGTTTTCAGG-3′
IFN-γ	5′-GAGGAACTGGCAAAAGGATG-3′	5′-TGAGCTCATTGAATGCTTGG-3′

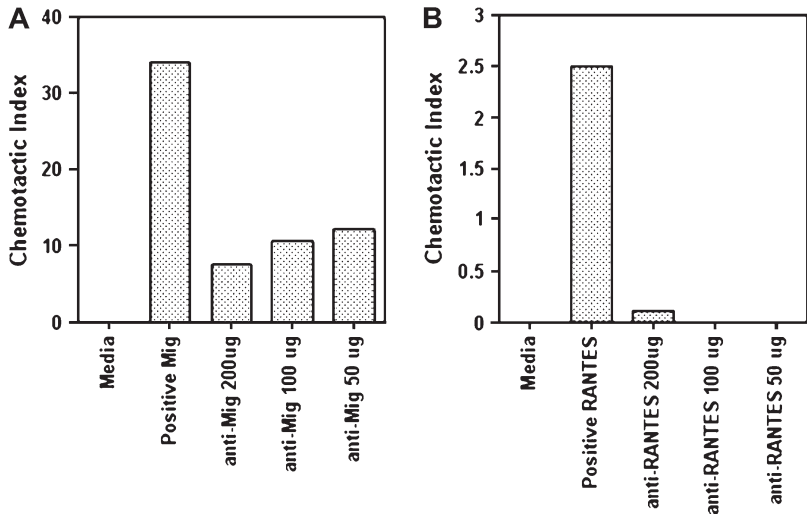

Fig. 1. Chemokine antisera inhibit lymphocyte migration *in vitro*. The ability of anti-MIG and anti-RANTES antisera to block cell migration was determined by utilizing a transwell chemotaxis assay. (A) Migration of $CXCR3^+$ 300-19 in response to recombinant mouse MIG was reduced by ~75% upon pre-incubation with anti-MIG antiserum at varying concentrations. (B) Activated splenocytes taken from mice immunized with MHV express the RANTES receptors CCR1 and CCR5 (55, 56). Migration of activated splenocytes in response to recombinant mouse RANTES was reduced to background levels following pre-incubation with varying concentrations of anti-RANTES antisera. Data are representative of two separate experiments.

IL-2 and IL-10 gene expression correlates with chemokine neutralization and virus expression

Anti-MIG and anti-RANTES antisera were administered individually to mice by intra-peritoneal injections starting at 10 days after infection with Theiler's virus. Analyses were conducted 1 month later. Since viral load and the immune responses triggered by virus are major factors regulating CNS pathology in this model, we looked for changes in mRNA levels for a variety of viral and immune-related genes. Real-time RT–PCR was performed with RNA isolated from homogenates of spinal cords and brain stems. Data from two, separate experiments were combined. In one experiment mice were treated with antiserum at 10 and 17 d.p.i. and analyzed at 56 d.p.i. (39 days post-treatment interval), and in the other experiment mice were treated once at 12 d.p.i. and analyzed at 48 d.p.i. (36 days post-treatment interval). Average RNA levels for most genes examined were not significantly affected by antiserum treatment, including VP2 viral capsid protein, CXCR3 chemokine receptor, IFN-γ, IL-2, IL-4 or GAPDH (Fig. 2). One exception was a modest increase in IL-10 mRNA by RANTES antiserum (Fig. 2D). When gene expression for each of these molecules was analyzed in the two experiments separately, only for IL-10 were mRNA levels different between treatment and control groups following two antiserum injections but not following a single injection. Thus, chemokine neutralization had few, lasting effects on the expression of immune-related genes.

More interestingly, we discovered important relationships among IL-2, IL-10 and VP2. Firstly, expression of IL-2 was inversely related to the expression of IL-10 ($r = -0.58$, $P < 0.0001$; Fig. 2E). Mice with high IL-2 levels had low IL-10 levels in the CNS, and vice versa. Secondly, analysis of the IL-2/IL-10 ratio revealed a shift toward IL-10 expression with anti-RANTES treatment ($P = 0.02$; Fig. 2F). Thirdly, we found that levels of both IL-2 and IL-10 correlated VP2. That is, IL-2 RNA decreased ($r = -0.50$, $P = 0.01$; Fig. 3A) and IL-10 increased ($r = 0.88$, $P < 0.0001$; Fig. 3B) in proportion to increasing levels of VP2 RNA. Finally, the IL-2/IL-10 ratio correlated strongly with levels of VP2 RNA ($r = -0.73$, $P < 0.0001$; Fig. 3C). Mice with the lowest ratio of IL-2/IL-10 had the highest levels of VP2. Interestingly, the cytokine RNA levels varied across only a 3-fold range (0.5 log units) while VP2 RNA levels varied across a 100-fold range (2 log units). Since these correlations were found independent of specific antiserum treatments, the results indicate close relationships between IL-2, IL-1, and virus expression within a larger context of virus–host interactions.

Chemokine neutralization increases viral antigen expression

We further examined the effect of RANTES or MIG neutralization on virus expression by immunohistochemical detection and quantitation of virus in spinal cord cross-sections (10 per animal). This type of analysis is the most informative measure of virulence, as viral antigen expression in the spinal cord has been shown to correlate with the extent of pathology in chronically infected mice (29–31). In contrast, infectious virus demonstrated by plaque assays starts to decline after 2 weeks of infection and is present only at very low levels in chronically infected mice, despite an abundance of viral antigen and RNA (29, 32). Mice were treated with antiserum on 12 and 18 d.p.i. and analyzed at 45 d.p.i. (27 days post-treatment interval). All mice had spinal cord pathology, despite some mice having very few infected cells in the sections that we sampled. Virus-infected cells were found exclusively in the white matter tracts of the spinal cord rather than the gray matter where neuronal cell bodies are located. Virus expression was measured first by counting the number of spinal cord quadrants with virus antigen-positive cells. This revealed that mice treated with MIG antiserum had a higher percentage of spinal cord quadrants with infected cells than mice treated with non-immune

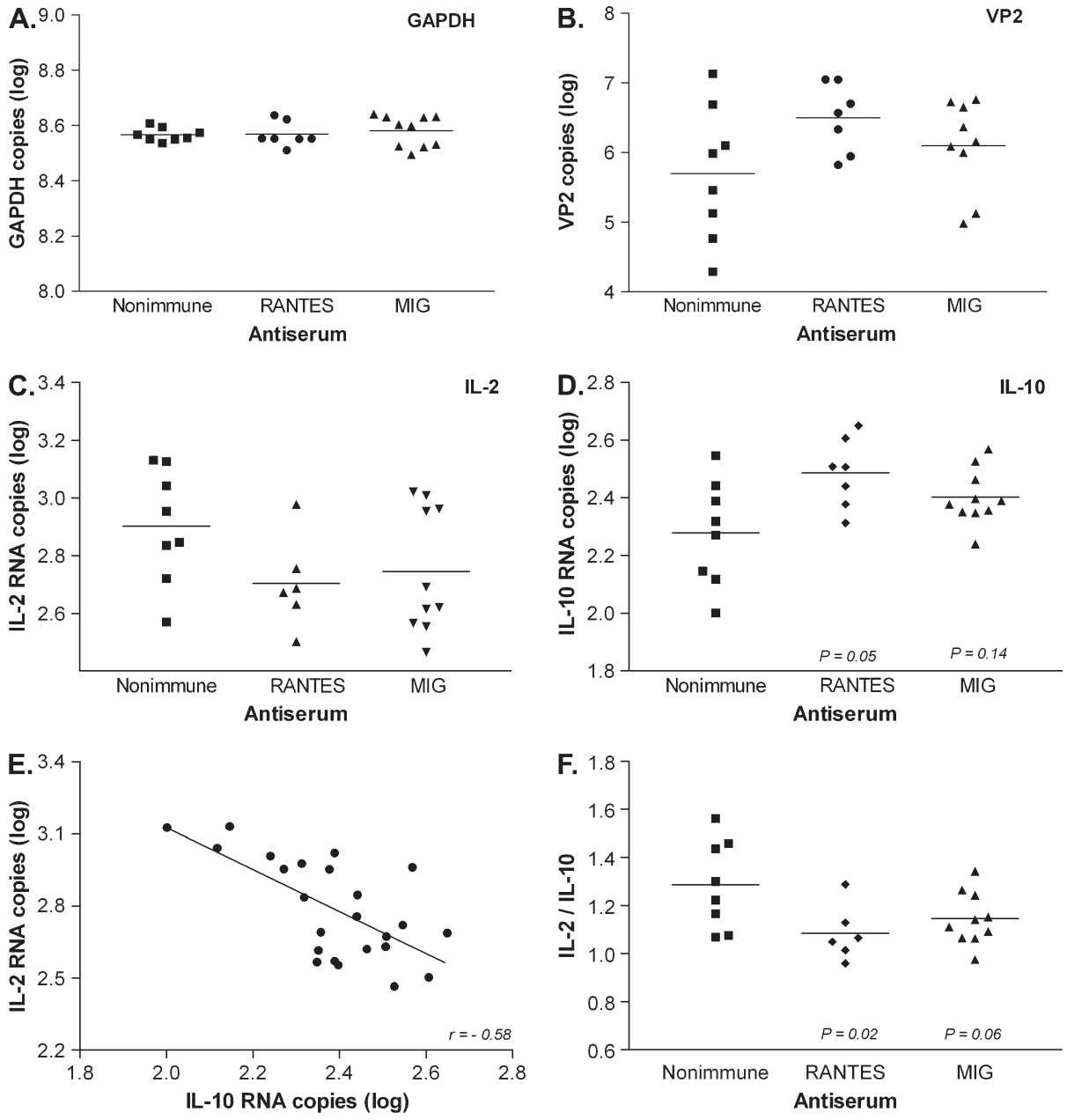

Fig. 2. Viral and cytokine gene expression following chemokine neutralization. Chemokine antisera were administered to mice once or twice between 10–17 d.p.i. RNA from spinal cords plus brain stems was isolated at 36 or 39 days following the end of treatment and analyzed by real-time RT–PCR. Data from two experiments are combined. GAPDH levels were used to validate equivalent RNA input (A). VP2 viral capsid (B) and IL-2 (C) were unchanged by the antisera treatments. IL-10 showed a statistically significant increase with anti-RANTES treatment (D). IL-2 and IL-10 levels were inversely related (E), and the IL-2/IL-10 ratio decreased in response to anti-RANTES (F).

serum ($P = 0.048$; Fig. 4A). We also analyzed viral antigen by counting the total number of infected cells as a function of spinal cord area and found that RANTES antiserum-treated mice had more infected cells relative to the area sampled, compared with control mice ($P = 0.048$; Fig. 4B). Thus, anti-MIG treatment resulted in a more widespread infection in the spinal cord white matter, whereas anti-RANTES treatment produced a higher overall level of virus expression. These findings indicate that both chemokines participate in the immune control of virus expression.

CD4 and CD8 expression patterns are unaltered by early chemokine neutralization

CD4 and CD8 T cells are important in the control against Theiler's virus, and the T_h1 subset of CD4 cells are the primary responders to RANTES and MIG (33–35). We examined the effects of chemokine neutralization on T cell infiltration by CD4 and CD8 immunostaining in spinal cord cross-sections. Mice were treated with antisera at Days 12 and 18 post-infection, a time at which lymphocyte infiltration is already present, then examined at 27 days post-treatment. T cells of both types were

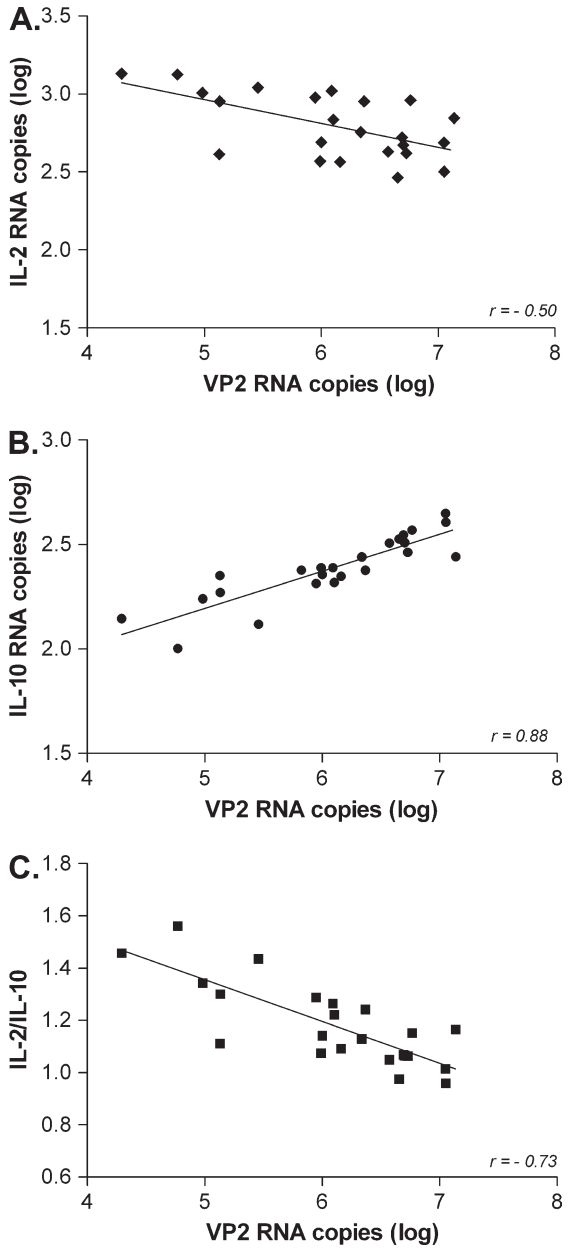

Fig. 3. IL-2 and IL-10 RNA levels correlate with virus expression. Data from Fig. 2 were examined for correlations with VP2. IL-2 and IL-10 varied across only a 3-fold range (0.5 log units), whereas VP2 varied across a 100-fold range (2 log units). IL-2 and the IL-2/IL-10 ratio declined (A, C), and IL-10 increased (B) in proportion to increasing VP2 levels.

present in all mice examined but neither their abundance nor the patterns of infiltration was obviously affected by MIG or RANTES antisera (Fig. 5). Lymphocytes infiltrated spinal cords extensively in all experimental groups and co-localized with virus-infected cells. CD4 lymphocytes were located in the perivasculature and the white matter parenchyma, whereas CD8 lymphocytes were found primarily in the white matter parenchyma. Due to the extent of infiltration, an accurate, quantitative analysis of infiltration could not be performed. However, from a qualitative perspective we conclude that

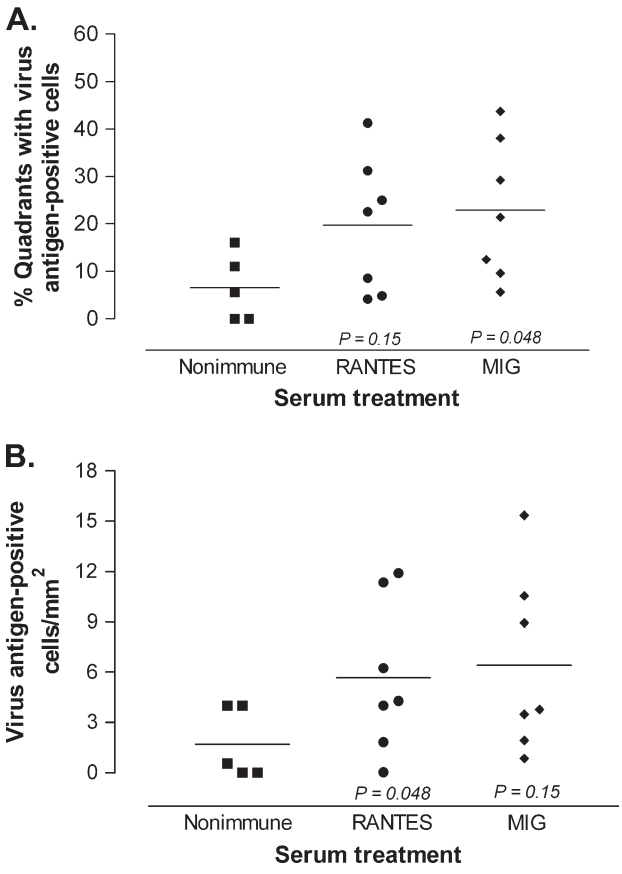

Fig. 4. Chemokine neutralization increases viral antigen expression in the spinal cord white matter. Mice were treated with the indicated serum at 12 and 18 d.p.i., and spinal cord cross-sections were immunostained for Theiler's virus at 30 days following the end of treatment. (A) MIG antiserum increased the number of spinal cord quadrants showing pathology, compared with control mice. (B) RANTES antiserum increased the total number of infected cells relative to the area sampled compared with control mice.

neutralization of MIG or RANTES did not have a significant or sustained effect on infiltration of inflammatory cells by 1-month post-treatment.

Chemokine neutralization increases spinal cord pathology

Our primary objective was to determine whether chemokine neutralization altered spinal cord pathology. Two similar experiments were conducted, and the data were combined. In the first experiment mice were treated at 12 d.p.i. and examined at 45 d.p.i. (27 days post-treatment interval). In the second experiment mice were treated at 12 and 18 d.p.i. and examined at 48 d.p.i. (36 days post-treatment interval). A systematic analysis of spinal cord cross-sections revealed differences in the amount and severity of pathology related to chemokine neutralization. In all experimental groups pathology was confined to the white matter and was characterized by varying degrees of lymphocyte and macrophage infiltration and myelin/axon destruction. Measurement of the percentage of spinal cord quadrants with lesions showed an increase in lesion frequency in mice treated with MIG antiserum (34% of quadrants) as compared with the non-immune serum group (20% of

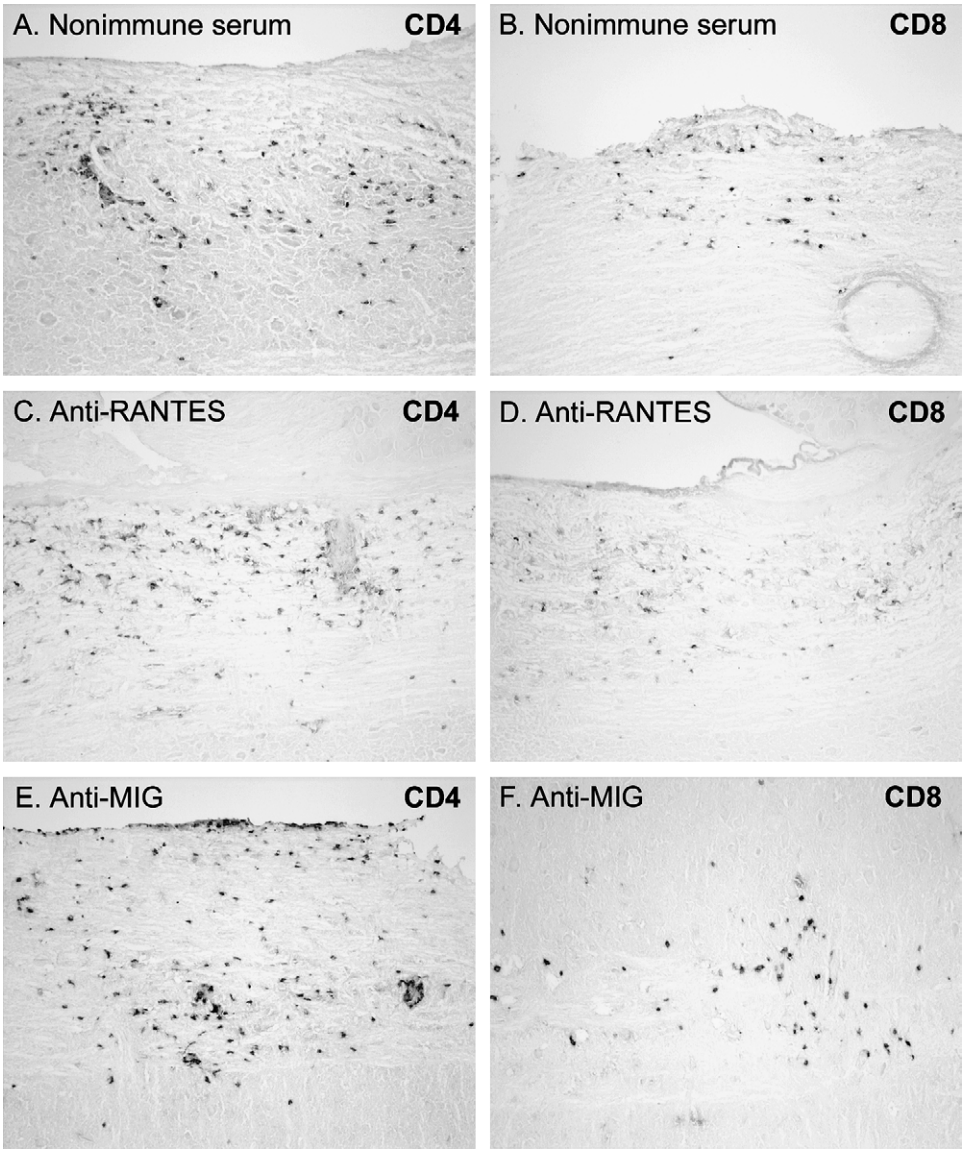

Fig. 5. Infiltration of CD4 and CD8 lymphocytes is normal in mice at 4 weeks following anti-chemokine treatment. Longitudinal spinal cord sections were immunostained for CD4 and CD8 at 27 days following the end of antiserum treatment. Large numbers of CD4 and CD8 lymphocytes were found in the white matter with similar distributions in mice treated with non-immune, anti-RANTES or anti-MIG serum.

quadrants; $P = 0.02$; Fig. 6A). Moreover, the percentage of spinal cord quadrants with inflammatory lesions was directly proportional to the percentage of quadrants with viral antigen, demonstrating the important relationship between spinal cord white matter pathology and viral antigen load (Fig. 6B).

We assessed spinal cord pathology further by grading the severity of each lesion on a 4-point scale using coded sections. As shown in Fig. 7, the lowest grade of pathology (Grade 1) consisted of mild lymphocyte infiltration without damage to the normal tissue architecture. Grade 2 pathology was characterized by mild lymphocyte plus macrophage infiltration and a small degree of demyelination. Grade 3 pathology was characterized by moderate lymphocyte and macrophage infiltration and significant demyelination. Grade 4 pathology comprised extensive inflammation and severe tissue destruction. In mice given non-immune serum, the most common lesions were Grade 1 and 2 (Fig. 7E). Grade 3 and 4 lesions together represented only 13% of the total lesions in control mice. In contrast, Grade 3 and 4 lesions together were three times more common in mice given RANTES antiserum, accounting for 35% of all lesions on average ($P = 0.03$ versus control group Grade 3 + 4 lesions combined). Twenty-three percent of lesions were Grade 3 or 4 after MIG neutralization, although this level was not statistically different from control mice. In conclusion, MIG neutralization resulted in an increase in the number of lesioned spinal cord quadrants, in similarity to the more widespread infection in these mice (previous section), whereas RANTES neutralization increased the overall severity of lesions, which correlated with a higher overall level of expression of virus antigen.

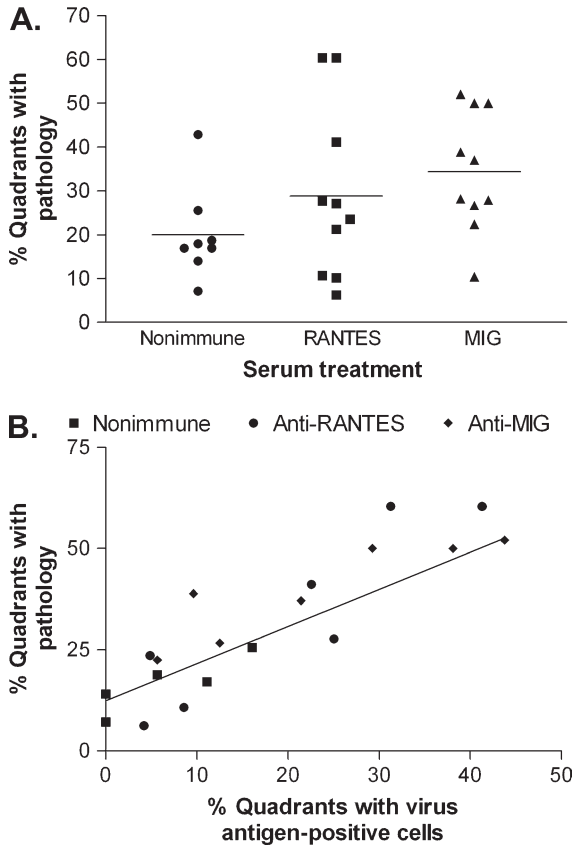

Fig. 6. Chemokine neutralization increases spinal cord white matter pathology. Infected mice were treated once or twice with the indicated serum between 12–18 d.p.i., and spinal cord cross-sections were examined at 27 or 36 days following the end of treatment. Data from both experiments were combined. (A) The percentage of spinal cord quadrants showing white matter pathology (4 quadrants per section and 10 sections per cord were examined) was higher following anti-MIG treatment as compared with control serum treatment. (B) The percentage of cord quadrants with white matte pathology correlated with the percentage of quadrants with infected cells.

Discussion

In the present report we demonstrate that RANTES and MIG regulate virus expression and spinal cord white matter pathology in the Theiler's virus-induced disease. Lymphocyte and macrophage infiltration into the CNS is vital for the control of TMEV but it also secondarily causes demyelination and axon destruction. The most logical hypothesis related to chemokine neutralization is that reducing immune cell infiltration would elicit a rise in virus but a decline in immunopathology. Looking at a time point when the consequences of antiserum treatment could be significantly manifested, we indeed found that RANTES neutralization and to a lesser extent MIG neutralization elevated virus expression but unexpectedly also caused more inflammation and demyelination in the spinal cord. These data suggest that immune activity in SJL mice attempts to restrict virus spread while limiting damage to normal tissues and that RANTES and MIG participate in the balancing of both these responses.

Many chemokines are produced during infection with the Daniel's strain of Theiler's virus (4, 6, 11). Expression starts within days of inoculation and lasts for several months in SJL and other susceptible strains of mice. One of the most abundantly produced chemokines, RANTES, is chemotactic for T cells and monocytes/macrophages, whereas MIG regulates migration of T cells but not monocytes (36). A comparison of Theiler's infection in a variety of mouse strains revealed that virus persistence is one of the major determinants of chemokine expression (11). Virus expression is also the major determinant of CNS pathology. The present study showed that virus antigen expression correlated with the extent of spinal cord demyelination, which supports similar findings at later stages of disease (29–31).

Considering these central roles for virus in inducing chemokine expression and pathology, we hypothesize that the principal effect of anti-RANTES and anti-MIG was to reduce infiltration of antiviral lymphocytes and/or monocytes and that pathology increased by 1-month post-treatment as a response to higher virus expression at the protein level. Activated CD4 cells with a T_h1 phenotype are the preferential targets of RANTES and MIG (33, 37, 38) and are also known to be important for virus control. Thus, a decline in antiviral activity is expected from anti-RANTES and anti-MIG treatments. Also in support of our hypothesis, virus titers and CNS pathology increase following antibody-mediated depletion or genetic knockout of CD4 lymphocytes (11, 23). Anti-chemokine treatments had subtler effects than total CD4 depletion, likely because a variety of chemokines contribute to infiltration of lymphocytes or macrophages during infection.

Virus titers increased at the level of virus antigen but not viral RNA. Trottier *et al.* (35) similarly found discordance between viral RNA, which remains high and relatively constant throughout the life of SJL mice, and infectious virus, which starts to decline as early as 3 weeks post-infection (32). Thus, viral RNA levels appear to be less responsive than virus antigen or infectious virus (plaques) to immunomodulation. An important question still to be resolved in the Theiler's field is the mechanism by which virus determines the extent of CNS pathology. One hypothesis is that TMEV causes direct cytolysis of CNS cells. The DA strain of Theiler's virus persists in oligodendrocytes, astrocytes and microglia/macrophages, but direct cytolysis of these cells appears to be limited (39, 40). In immunostained spinal cord sections we found only occasional, highly distended, infected cells. In addition, immunocompromised RAG−/− mice infected with Theiler's virus do not show significant demyelination prior to death at 3 weeks post-infection, even when virus is injected directly into the spinal cord, implying a limited degree of cytolysis (M.R. unpublished observations).

The more likely explanation is that the extent of virus expression determines the strength of the immune reaction, which in turn elicits secondary injury to myelin and other CNS cells. One of the best examples of this mechanism involves the adoptive transfer of immunocompetent splenocytes into infected, immunodeficient SCID mice (41). Increasing the number of transferred splenocytes is able to prevent TMEV-induced mortality but also increases immunopathology. Whereas transfer of very high numbers of splenocytes can clear virus in SCID mice, SJL mice typically are unable to clear Theiler's virus. Lymphocytes reactive to the major Theiler's virus epitopes are rare in SJL and other susceptible mouse

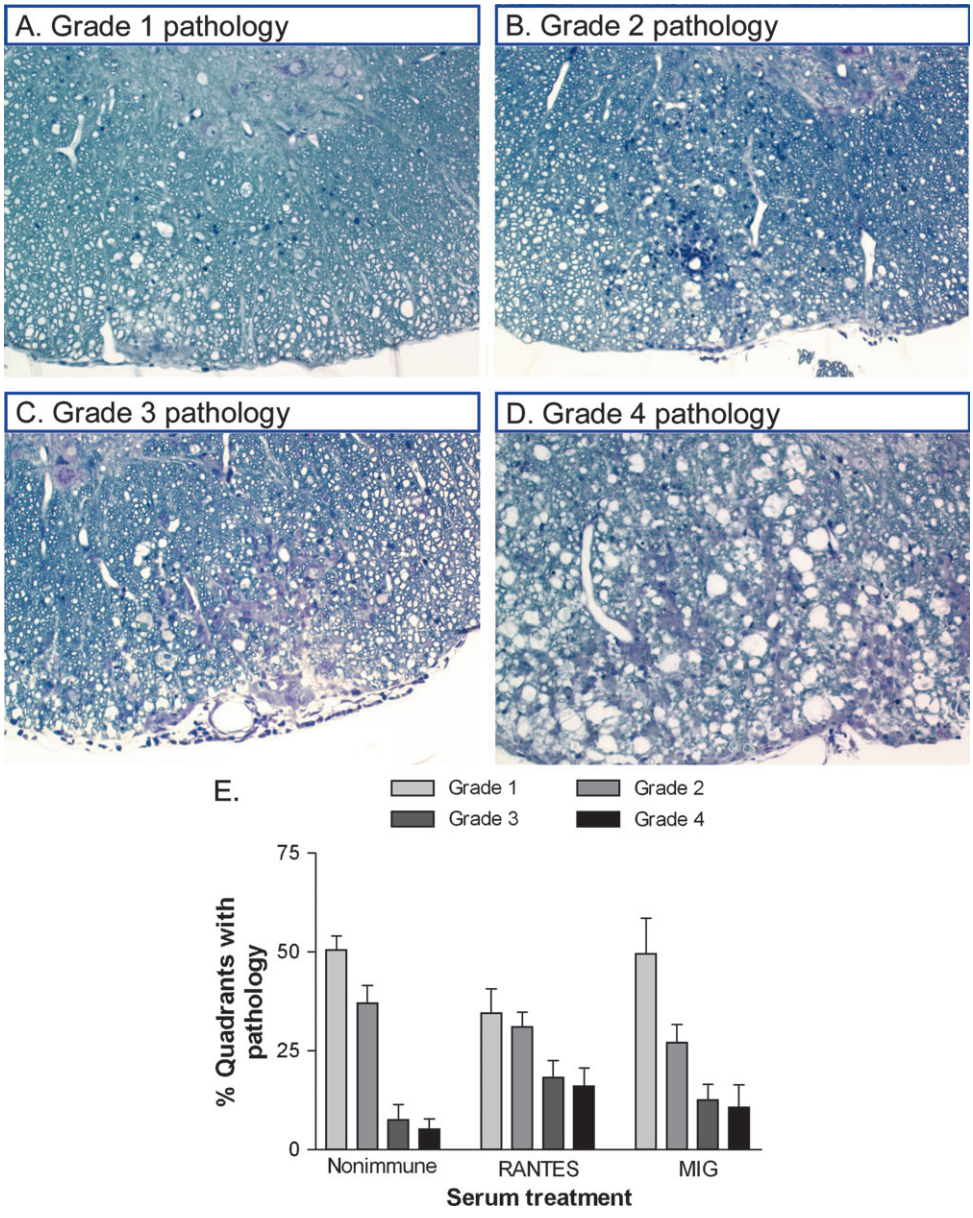

Fig. 7. Spinal cord pathology in infected mice. (A–D) Plastic-embedded, spinal cord sections were histologically stained to show lymphocyte and macrophage infiltration, demyelination and damage to the CNS. Sections were coded to blind the observer to treatment group and scored, based on the following scheme: Grade 1 = mild inflammation; Grade 2 = moderate inflammation; Grade 3 = mild–severe inflammation with moderate demyelination; Grade 4 = severe inflammation, demyelination and tissue damage. (E) Quantitative data shows that moderate to severe lesions (Grade 3 and 4 combined) were more abundant following anti-RANTES treatment as compared with control serum treatment ($P = 0.03$) but not following anti-MIG treatment ($P = 0.14$ versus control group Grade 3 + 4).

strains, in contrast to resistant strains such as C57BL/10 mice (15). The virus-specific response of only a minority of lymphocytes might partially explain why we did not observe obvious alterations in CD4 or CD8 lymphocyte infiltration by immunostaining. Another possible explanation is that a significant number of infiltrating lymphocytes or monocytes/macrophages might have been responding secondarily to tissue damage or might have had affinities for other chemokines. We also recognize that chemokine-neutralizing activity might have subsided over time and that specific lymphocyte infiltration might have rebounded by 1-month post-treatment.

The inverse relationships between IL-2 and IL-10 RNA levels and the correlations of both cytokines with viral RNA were intriguing, especially since IL-2 and IL-10 RNA varied only across a 3-fold range whereas virus varied across a 100-fold range. Finding strong correlations within this context suggests that the changes in IL-2 and IL-10 were biologically relevant. A narrow window of regulation might explain why it has been difficult to associate the various aspects of Theiler's disease (e.g. susceptibility versus resistance) or multiple sclerosis (e.g. inactive versus active) with particular cytokine profiles (42–50). It is tempting to speculate that these changes were indicative of

the proportions of T_h1 and T_h2 lymphocytes. For example, an increase in virus concurrent with a decrease in IL-2 is consistent with the hypothesis that IL-2-expressing T_h1 lymphocytes are important for virus control. However, a suitable explanation probably is more complicated because two other cytokines representative of T_h1 and T_h2 lymphocytes, IFN-γ and IL-4, did not show correlations with viral RNA. Glial cells also express many of these cytokines as well as the chemokine receptor, CXCR3, which confounds conclusions about the specific responses of infiltrating cells (51–54).

The major implication from our study is that even short-term modulation of the immune response can significantly influence spinal cord pathology in the long term. A question for future studies is whether the increases in virus expression and pathology are sustained, or whether antiviral mechanisms are able to reduce these parameters back to a level characteristic of untreated mice. Another question is whether more neurological dysfunction eventually develops in mice in which chemokines are neutralized. Chemokine neutralization, although not immediately impacting function, may accelerate the onset and eventual severity of deficits. From the standpoint of human disease, chemokine neutralization represents a promising therapy for autoimmune diseases where lymphocyte dysregulation and autoreactivity are the primary etiologies. In contrast, our findings caution against the use of chemokine neutralization where viral etiologies are suspected. Even mild and apparently benign treatments may have adverse effects later in disease.

Acknowledgements

The authors acknowledge the technical support of Laurie Zoecklein, Louisa Papke and Jeff Gamez. This work was supported by grants from NIH (NS32129 and NS38468).

Abbreviations

CNS	central nervous system
d.p.i.	days post-infection
DA	Daniel's strain of Thelier's virus
IP-10	interferon-γ inducible protein-10
MHV	mouse hepatitis virus
MIG	monokine induced by IFN-γ
p.f.u.	plaque-forming unit
RANTES	regulated on activation, normal T cell expressed and secreted
RT	reverse transcriptase
TMEV	Theiler's murine encephalomyelitis virus

References

1 Charles, P. C., Chen, X., Horwitz, M. S. and Brosnan, C. F. 1999. Differential chemokine induction by the mouse adenovirus type-1 in the central nervous system of susceptible and resistant strains of mice. *J. Neurovirol.* 5:55.
2 Hoffman, L. M., Fife, B. T., Begolka, W. S., Miller, S. D. and Karpus, W. J. 1999. Central nervous system chemokine expression during Theiler's virus-induced demyelinating disease. *J. Neurovirol.* 5:635.
3 Manchester, M., Eto, D. S. and Oldstone, M. B. 1999. Characterization of the inflammatory response during acute measles encephalitis in NSE-CD46 transgenic mice. *J. Neuroimmunol.* 96:207.
4 Murray, P. D., Krivacic, K., Chernosky, A., Wei, T., Ransohoff, R. M. and Rodriguez, M. 2000. Biphasic and regionally-restricted chemokine expression in the central nervous system in the Theiler's virus model of multiple sclerosis. *J. Neurovirol.* 6 (Suppl. 1) :S44.
5 Nansen, A., Marker, O., Bartholdy, C. and Thomsen, A. R. 2000. CCR2+ and CCR5+ CD8+ T cells increase during viral infection and migrate to sites of infection. *Eur. J. Immunol.* 30:1797.
6 Theil, D. J., Tsunoda, I., Libbey, J. E., Derfuss, T. J. and Fujinami, R. S. 2000. Alterations in cytokine but not chemokine mRNA expression during three distinct Theiler's virus infections. *J. Neuroimmunol.* 104:22.
7 Liu, M. T., Armstrong, D., Hamilton, T. A. and Lane, T. E. 2001. Expression of Mig (monokine induced by interferon-gamma) is important in T lymphocyte recruitment and host defense following viral infection of the central nervous system. *J. Immunol.* 166:1790.
8 Lokensgard, J. R., Hu, S., Sheng, W. *et al.* 2001. Robust expression of TNF-alpha, IL-1beta, RANTES, and IP-10 by human microglial cells during nonproductive infection with herpes simplex virus. *J. Neurovirol.* 7:208.
9 Palma, J. P. and Kim, B. S. 2001. Induction of selected chemokines in glial cells infected with Theiler's virus. *J. Neuroimmunol.* 117:166.
10 Peterson, K. E., Robertson, S. J., Portis, J. L. and Chesebro, B. 2001. Differences in cytokine and chemokine responses during neurological disease induced by polytropic murine retroviruses Map to separate regions of the viral envelope gene. *J. Virol.* 75:2848.
11 Ransohoff, R. M., Wei, T., Pavelko, K. D., Lee, J. C., Murray, P. D. and Rodriguez, M. 2002. Chemokine expression in the central nervous system of mice with a viral disease resembling multiple sclerosis: roles of CD4+ and CD8+ T cells and viral persistence. *J. Virol.* 76:2217.
12 Liu, M. T., Chen, B. P., Oertel, P. *et al.* 2000. The T cell chemoattractant IFN-inducible protein 10 is essential in host defense against viral-induced neurologic disease. *J. Immunol.* 165:2327.
13 Liu, M. T., Chen, B. P., Oertel, P. *et al.* 2001. The CXC chemokines IP-10 and Mig are essential in host defense following infection with a neurotropic coronavirus. *Adv. Exp. Med. Biol.* 494:323.
14 Liu, M. T., Keirstead, H. S. and Lane, T. E. 2001. Neutralization of the chemokine CXCL10 reduces inflammatory cell invasion and demyelination and improves neurological function in a viral model of multiple sclerosis. *J. Immunol.* 167:4091.
15 Lin, X., Pease, L. R., Murray, P. D. and Rodriguez, M. 1998. Theiler's virus infection of genetically susceptible mice induces central nervous system-infiltrating CTLs with no apparent viral or major myelin antigenic specificity. *J. Immunol.* 160:5661.
16 Croxford, J. L., Olson, J. K. and Miller, S. D. 2002. Epitope spreading and molecular mimicry as triggers of autoimmunity in the Theiler's virus-induced demyelinating disease model of multiple sclerosis. *Autoimmun. Rev.* 1:251.
17 McGavern, D. B., Murray, P. D., Rivera-Quinones, C., Schmelzer, J. D., Low, P. A. and Rodriguez, M. 2000. Axonal loss results in spinal cord atrophy, electrophysiological abnormalities and neurological deficits following demyelination in a chronic inflammatory model of multiple sclerosis. *Brain* 123:519.
18 Ure, D. R. and Rodriguez, M. 2002. Preservation of neurologic function during inflammatory demyelination correlates with axon sparing in a mouse model of multiple sclerosis. *Neuroscience* 111:399.
19 Tannenbaum, C. S., Tubbs, R., Armstrong, D., Finke, J. H., Bukowski, R. M. and Hamilton, T. A. 1998. The CXC chemokines IP-10 and Mig are necessary for IL-12-mediated regression of the mouse RENCA tumor. *J. Immunol.* 161:927.
20 Lane, T. E., Liu, M. T., Chen, B. P. *et al.* 2000. A central role for CD4(+) T cells and RANTES in virus-induced central nervous system inflammation and demyelination. *J. Virol.* 74:1415.
21 Hunter, S. F., Miller, D. J. and Rodriguez, M. 1997. Monoclonal remyelination-promoting natural autoantibody SCH 94.03: pharmacokinetics and *in vivo* targets within demyelinated spinal cord in a mouse model of multiple sclerosis. *J. Neurol. Sci.* 150:103.

22 Pirko, I., Ciric, B. Gamez, J. *et al.* 2004. A human monoclonal antibody that promotes remyelination enters the CNS and decreases lesion load as detected by T2 weighted spinal cord MRI in a virus-induced murine model of MS. *FASEB J.* 18:1577.
23 Rodriguez, M., and Sriram, S. 1988. Successful therapy of Theiler's virus-induced demyelination (DA strain) with monoclonal anti-Lyt-2 antibody. *J. Immunol.* 140:2950.
24 Glass, W. G. and Lane, T. E. 2003. Functional analysis of the CC chemokine receptor 5 (CCR5) on virus-specific CD8+ T cells following coronavirus infection of the central nervous system. *Virology* 312:407.
25 Glass, W. G. and Lane, T. E. 2003. Functional expression of chemokine receptor CCR5 on CD4(+) T cells during virus-induced central nervous system disease. *J. Virol.* 77:191.
26 Proost, P., Schutyser, E., Menten, P. *et al.* 2001. Amino-terminal truncation of CXCR3 agonists impairs receptor signaling and lymphocyte chemotaxis, while preserving antiangiogenic properties. *Blood* 98:3554.
27 Pierce, M. L. and Rodriguez, M. 1989. Erichrome stain for myelin on osmicated tissue embedded in clycol methacrylate plastic. *J. Histotechnol.* 12:35.
28 Rodriguez, M., Leibowitz, J. L. and Lampert, P. W. 1983. Persistent infection of oligodendrocytes in Theiler's virus-induced encephalomyelitis. *Ann. Neurol.* 13:426.
29 Lipton, H. L., Kratochvil, J., Sethi, P. and Dal Canto, M. C. 1984. Theiler's virus antigen detected in mouse spinal cord 2 1/2 years after infection. *Neurology* 34:1117.
30 Chamorro, M., Aubert, C., and Brahic, M. 1986. Demyelinating lesions due to Theiler's virus are associated with ongoing central nervous system infection. *J. Virol.* 57:992.
31 Rodriguez, M. and Lindsley, M. D. 1992. Immunosuppression promotes CNS remyelination in chronic virus-induced demyelinating disease. *Neurology* 42:348.
32 Trottier, M., Kallio, P., Wang, W. and Lipton, H. L. 2001. High numbers of viral RNA copies in the central nervous system of mice during persistent infection with Theiler's virus. *J. Virol.* 75:7420.
33 Siveke, J. T. and Hamann, A. 1998. T helper 1 and T helper 2 cells respond differentially to chemokines. *J. Immunol.* 160:550.
34 Kennedy, K. J. and Karpus, W. J. 1999. Role of chemokines in the regulation of Th1/Th2 and autoimmune encephalomyelitis. *J. Clin. Immunol.* 19:273.
35 Moser, B. and Loetscher, P. 2001. Lymphocyte traffic control by chemokines. *Nat. Immunol.* 2:123.
36 Glass, W. G., Chen, B. P., Liu, M. T. and Lane, T. E. 2002. Mouse hepatitis virus infection of the central nervous system: chemokine-mediated regulation of host defense and disease. *Viral Immunol.* 15:261.
37 Kennedy, K. J. and Karpus, W. J. 1999. Role of chemokines in the regulation of Th1/Th2 and autoimmune encephalomyelitis. *J. Clin. Immunol.* 19:273.
38 Moser, B. and Loetscher, P. 2001. Lymphocyte traffic control by chemokines. *Nat. Immunol.* 2:123.
39 Graves, M. C., Bologa, L., Siegel, L. and Londe, H. 1986. Theiler's virus in brain cell cultures: lysis of neurons and oligodendrocytes and persistence in astrocytes and macrophages. *J. Neurosci. Res.* 15:491.
40 Qi, Y. and Dal Canto, M. C. 1996. Effect of Theiler's murine encephalomyelitis virus and cytokines on cultured oligodendrocytes and astrocytes. *J. Neurosci. Res.* 45:364.
41 Rodriguez, M., Pavelko, K. D., Njenga, M. K., Logan, W. C. and Wettstein, P. J. 1996. The balance between persistent virus infection and immune cells determines demyelination. *J. Immunol.* 157:5699.
42 Morris, M. M., Dyson, H., Baker, D., Harbige, L. S., Fazakerley, J. K. and Amor, S. 1997. Characterization of the cellular and cytokine response in the central nervous system following Semliki Forest virus infection. *J. Neuroimmunol.* 74:185.
43 Parra, B., Hinton, D. R., Lin, M. T., Cua, D. J. and Stohlman, S. A. 1997. Kinetics of cytokine mRNA expression in the central nervous system following lethal and nonlethal coronavirus-induced acute encephalomyelitis. *Virology* 233:260.
44 Sato, S., Reiner, S. L., Jensen, M. A. and Roos, R. P. 1997. Central nervous system cytokine mRNA expression following Theiler's murine encephalomyelitis virus infection. *J. Neuroimmunol.* 76:213.
45 Hatalski, C. G., Hickey, W. F., and Lipkin, W. I. 1998. Evolution of the immune response in the central nervous system following infection with Borna disease virus. *J. Neuroimmunol.* 90:137.
46 Link, H. 1998. The cytokine storm in multiple sclerosis. *Mult. Scler.* 4:12.
47 Baranzini, S. E., Elfstrom, C., Chang, S. Y. *et al.* 2000. Transcriptional analysis of multiple sclerosis brain lesions reveals a complex pattern of cytokine expression. *J. Immunol.* 165:6576.
48 Chang, J. R., Zaczynska, E., Katsetos, C. D., Platsoucas, C. D. and Oleszak, E. L. 2000. Differential expression of TGF-beta, IL-2, and other cytokines in the CNS of Theiler's murine encephalomyelitis virus-infected susceptible and resistant strains of mice. *Virology* 278:346.
49 Franciotta, D., Zardini, E., Bergamaschi, R., Andreoni, L. and Cosi, V. 2000. Interferon-gamma and interleukin-4-producing T cells in peripheral blood of multiple sclerosis patients. *Eur. Cytokine Netw.* 11:677.
50 Rodriguez-Sainz, M. C., Sanchez-Ramon, S., de Andres, C., Rodriguez-Mahou, M. and Munoz-Fernandez, M. A. 2002. Th1/Th2 cytokine balance and nitric oxide in cerebrospinal fluid and serum from patients with multiple sclerosis. *Eur. Cytokine Netw.* 13:110.
51 Jander, S., Pohl, J., D'Urso, D., Gillen, C. and Stoll, G. 1998. Time course and cellular localization of interleukin-10 mRNA and protein expression in autoimmune inflammation of the rat central nervous system. *Am. J. Pathol.* 152:975.
52 Dorf, M. E., Berman, M. A., Tanabe, S., Heesen, M. and Luo, Y. 2000. Astrocytes express functional chemokine receptors. *J. Neuroimmunol.* 111:109.
53 Hulshof, S., Montagne, L., De Groot, C. J. and Van, D. V. 2002. Cellular localization and expression patterns of interleukin-10, interleukin-4, and their receptors in multiple sclerosis lesions. *GLIA* 38:24.
54 Flynn, G., Maru, S., Loughlin, J., Romero, I. A. and Male, D. 2003. Regulation of chemokine receptor expression in human microglia and astrocytes. *J. Neuroimmunol.* 136:84.
55 Glass, W. G. and Lane, T. E. 2003. Functional analysis of the CC chemokine receptor 5 (CCR5) on virus-specific CD8+ T cells following coronavirus infection of the central nervous system. *Virology* 312:407.
56 Glass, W. G. and Lane, T. E. 2003. Functional expression of chemokine receptor CCR5 on CD4(+) T cells during virus-induced central nervous system disease. *J. Virol.* 77:191.